Proceedings of ERAD 2006

Hydrometeor supervised classification using a bistatic C-band weather radar configuration

D. Scaranari[1], F. S. Marzano[1,2], G. Vulpiani[2,3], M. Montopoli[2], M. Celano[4], P. P. Alberoni[4]

[1] DIE, University of Rome "La Sapienza", Rome (Italy).

[2] CETEMPS, L'Aquila (Italy).

[3] MeteoFrance, Trappes (France).

[4] ARPA-SIM, Bologna (Italy).

1 Introduction

Dual-polarized weather coherent radar systems can offer the opportunity to detect and identify different classes of hydrometeors in liquid, mixed and ice phases usually present in stratiform and convective storms. This important and appealing capability depends on the fact that dual-polarized radar measurements, such as the co-polar reflectivity Z_{hh}, the differential reflectivity Z_{dr} and the specific differential phase K_{dp}, are highly sensitive to physical properties of hydrometeors like composition, size, shape and orientation [Vivekanandan et al. (1999), Straka et al. (2000)].

Most scientific literature about hydrometeor classification has been so far devoted to classification techniques designed for S-band dual-polarized weather radars [Zrnić et al. (2001), Lim et al. (2005), Ryzhkov et al. (2005)]. Only recently some works related to the exploitation of C-band measurements for hydrometeor classification have been presented [Keenan (2003), Baldini et al. (2004), Galletti et al. (2005), Marzano et al. (2006)]. The interest of assessing C-band hydrometeor classification may also emerge from the consideration that most mid-to-high latitude weather radars operate and are planned at C-band [Alberoni et al. (2002)]. On the other hand rainfall path attenuation cannot be disregarded when inverting radar measurements at C-band frequencies and above [Bringi and Chandrasekar (2001), Iguchi and Meneghini (1994)]. Differential phase shift measurements can be exploited to correct for precipitation path attenuation effects in a fairly effective way [Testud et al. (2000), Vulpiani et al. (2005)], even though large statistical fluctuations and residual ambiguities may affect the overall accuracy.

In this work a model-trained supervised fuzzy-logic radar algorithm for hydrometeor classification at C-band (FRAHCC) is presented. The goal is not to devise a new fuzzy logic algorithm, but using an established approach to: i) extend it from S-band to C-band radar data; ii) handle both power and phase measurements giving some details of the approach at C-band; iii) show the improvements obtained using a C-band tuned algorithm with respect to an S-band based approach; iv) evaluate the impact of path-integrated attenuation (PIA) exploiting a bistatic radar configuration.

Correspondence to: Frank S. Marzano.

marzano@die.uniroma1.it

2 Hydrometeor radar scattering model at C-band

We limit our attention to copolar reflectivity Z_{hh}, differential reflectivity Z_{dr} and specific differential phase K_{dp}. The analysis of co-polar correlation coefficient ρ_{hv} and linear depolarization ratio L_{dr} is beyond our scopes. Once the particle shape, orientation and dielectric composition together with particle size distribution $N(D_e)$ are known, a numerical solution can be adopted to derive both $\sigma_{hh,vv}$ and $f_{hh,vv}$. The T-Matrix method is an effective numerical solution of the scattering problem for non-spherical particles by means of the electromagnetic equivalence theorem.

A correct microphysical and dielectric modeling of hydrometeors is essential to obtain meaningful simulations of polarimetric radar measurements [Beard and Chuang (1987)]. Detailed information about several hydrometeor types can be found in Straka et al. (2000) and here we basically follow their approach. However, in this work only 10 hydrometeor classes have been established as follows: LD (*large drops*), LR (*light rain*), MR (*medium rain*), HR (*heavy rain*), H/R (*hail/rain mixture*), H (*hail*), G/SH

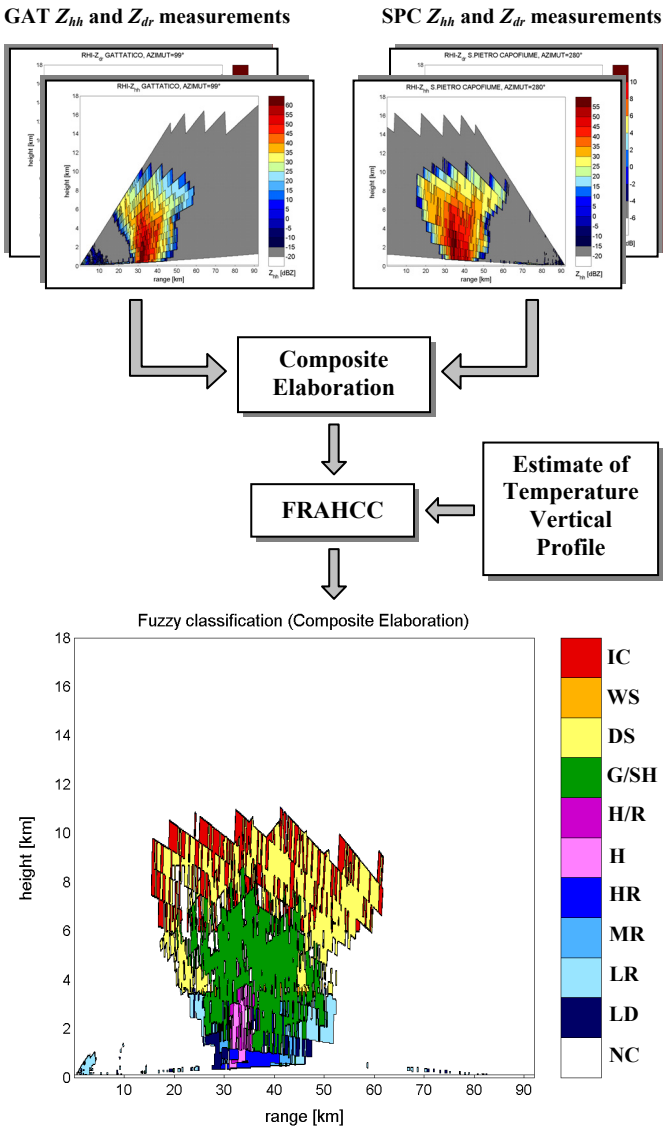

Fig. 1. Composite elaboration scheme with FRAHCC application to the RHI section corresponding to the conjunction line GAT-SPC. Radar data refer to 2003, 20th of May, 16:34 GMT.

(*graupel/small hail*), DS (*dry snow*), WS (*wet snow*), IC (*ice crystals*). Possible temperature ranges for the ten different hydrometeor classes have been derived from Zrnić et al. (2001). In this work we have assumed that all particle shapes may be approximated by spheroids. The size distribution of each hydrometeor has been modeled through a normalized Gamma. Water and ice dielectric constants are derived from Ray's (1972) and Warren's (1984) models, respectively. Ten sets of 300 scattering simulations for each hydrometeor class have been carried out in order to have statistically significant simulated polarimetric signatures.

With respect to S-band measurements, C-band signatures are more sensitive to shapes and, in general, present larger values of Z_{dr} and K_{dp} and lower values of co-polar correlation [Zrnić et al. (2001)]. Most relevant differences between the two band behaviors have been found for LD, MR, HR and H/R classes. Specifically, it is worth noting that Z_{dr} at S-band is not usually larger than 3.5 dB, while at C-band LD and HR give rise to Z_{dr} even larger than 5 dB. The key advantage of K_{dp} at C-band is the capability to discriminate between rain and ice hydrometors, but unfortunately the retrieval of K_{dp} is affected by the backscattering differential phase shift δ_{hv}, which is no more negligible at C-band [Iguchi and Meneghini (1994), Bringi and Chandrasekar (2001)].

3 Fuzzy-logic classification method

As previously noted, at C-band path attenuation is relevant and cannot be neglected. All these aspects make fuzzy logic one of the best solutions for the hydrometeor classification problem [Lim et al. (2005)]. Fuzzy-logic techniques are fairly simple and flexible to set up and their behavior tends to be robust to noisy data [Bringi and Chandrasekar (2001)]. A fuzzy logic system basically provides a non-linear mapping of input data vectors into scalar outputs. Any fuzzy-logic algorithm consists of three main stages: *i*) fuzzification; *ii*) inference; *iii*) de-fuzzification [Lim et al. (2005)]. In this work we have considered, as input data vector, the combination of reflectivity Z_{hh}, differential reflectivity Z_{dr} and environmental temperature T. This choice is mainly dictated by the bistatic radar system used for algorithm testing. In order to generalize the C-band methodology to polarimetric radars, we have also considered the possible use of specific differential phase K_{dp}.

In the standard FRAHCC technique the fuzzification stage is characterized by 10 bi-dimensional membership functions (MBFs) for Z_{hh} and Z_{dr} and 10 mono-dimensional MBFs for temperature. Temperature for every radar bin is evaluated by means of a vertical radio-sounding profile realized in proximity of the storm. In absence of this kind of measurement, a standard temperature gradient can be assumed as a first approximation. Definition of MBFs is a fundamental task that affects the classification accuracy. The starting point has been a set of MBFs, originally described in Straka et al. (2000), usually referred as the fuzzy-logic scheme developed for the National Severe Storm Laboratory (NSSL) polarimetric radars at S-band [Zrnić et al. (2001)]. MBFs adopted in this work have trapezoidal forms and analytical expressions have been derived by means of accurate observations of T-Matrix simulations at C-band. Linear fuzzy thicknesses can be different for each hydrometeor class. Temperature MBFs are also trapezoidal functions, directly derived from Zrnić et al. (2001). The inference rule (I_{Ri}) for the *i-th* class is based on the product of membership degrees, derived from MBFs as it follows when only Z_{hh} and Z_{dr} are available:

$$I_{Ri} = M_{Zi}(Z_{hh}, Z_{dr}) M_{Ti}(T) \qquad (1)$$

where i=0-9, the M_{Zi} and M_{Ti} are the MBFs for (Z_{hh}, Z_{dr}) and T of the *i-th* class. The choice of product, instead of linear combination, has the purpose to limit classification errors as far as possible: if, for a given class, one measurement is significantly out of range, the low value of the corresponding MBF will definitely suppress the class.

The defuzzification is carried out by a maximum-value rule applied to (1) giving the estimated hydrometeor class index i_c which the radar bin is assigned to:

$$\hat{i}_c = Max_i\left[I_{Ri}\right] \quad i = 0,1,...,9 \tag{2}$$

where Max_i is the maximum operator with respect to the *i-th* class. If two or more rules present the same maximum value, NC (*not classified*) label is assigned to the radar bin.

In order to evaluate the expected classification accuracy, we have generated a training and test data set consisting of 300 independent simulations of $Z_{hh,}$, $Z_{dr,}$ and K_{dp} for each hydrometeor class, with the environmental temperature T uniformly distributed inside specific intervals. Radar measurements at C-band have been simulated by adding a zero-mean Gaussian noise to data with standard deviations equal to 1 dBZ, 0.3 dB and 0.2°/km for Z_{hh}, Z_{dr} and K_{dp}, respectively.

Contingency tables, also known as confusion matrices, are used to evaluate classification accuracy on either real or synthetic data. For comparison, classification results using S-band MBFs have been computed. Improvements of the hydrometeor classification accuracy w.r.t. the use of S-band designed MBFs [Baldini et al. (2004)], measured in terms of overall accuracy (OA) and average non-classified samples percentage (NC_{av}), are noteworthy: OA rises from 48% to 62%, while NC_{av} decreases from 26% to 15%.

4 Case study

Available radar data refer to a convective episode occurred in the region between two dual-polarized C-band radar systems GPM-500C, both located in the Po valley and about 90 km apart: the S. Pietro Capofiume (SPC) and the Gattatico (GAT) radars, both managed by ARPA-SIM Emilia-Romagna. Details about the radar systems and the evolution of the convective event are given by Alberoni et al. (2001), Alberoni et al. (2002), Marzano et al. (2006).

Reflectivity and differential reflectivity data available from the two radars GAT and SPC have been first classified with the previously described FRAHCC technique, disregarding path-attenuation effects. Temperature vertical average profile has been retrieved from a vertical radio-sounding made at SPC meteorological station. Since truth data regarding the storm on the connection line are unavailable, only qualitative tests can be carried out. This visual inspection is aimed at evaluating the microphysical consistency of the hydrometeor field and the information content of each algorithmic choice [Zrnić et al. (2001)]. Accuracy improvements can be recognized by direct observations of the RHI diagrams, first with S-band MBFs and then with C-band MBFs. In the latter case the number of non-classified (NC) radar bins considerably decreases, and ice crystals detection (IC) is performed in a more realistic way. Classification results are also physically self-consistent: the hail core (H and H/R) is correctly detected at the centre of the convective storm, graupel (G/SH) is reasonably identified all around the hail core, rain is present only at low altitude while snow and ice crystals (DS, WS, IC) are properly found within the top layers of the storm.

In order to correct for path integrated attenuation (PIA), since differential phase shift measurements are unavailable we can exploit the bistatic radar observation of this convective event by either using a composite field approach or a constrained inversion algorithm [Iguchi and Meneghini (1994), Vulpiani et al. (2005)].

When a bistatic observation of a storm is available, the path integrated attenuation (PIA) can be estimated by looking at the differences between the attenuated measured reflectivity Z_{hhm}, observed from the considered radar, and the non-attenuated reflectivity Z_{hh}, observed by the other radar at the rain-cloud edge. Let us consider the line connecting the SPC and GAT radars at the lowest elevation angle θ_0=0.5°. Along this line, an average over 2.5 km (10 range bins) gives a value of 5 ± 2.4 dBZ for the radar reflectivity difference (Z_{hhm}^{GAT}-Z_{hhm}^{SPC}) and 7.5 ± 1.5 dBZ for (Z_{hhm}^{SPC}-Z_{hhm}^{GAT}). The average value between these two estimates seems to indicate a PIA of about 6.25 dB. In order to reconstruct the equivalent reflectivity range profiles of Z_{hh} and Z_{dr}, we can apply a set of path-attenuation correction algorithms with PIA constraint [Iguchi and Meneghini (1994), Testud et al. (2000), Vulpiani et al. (2005)]. Main problems are that radar data are quite noisy and fluctuating, the two radars may suffer for a different miscalibration and instrumental noise so that the estimate of PIA may be affected by a significant uncertainty. Moreover the various correction algorithms may give different results. In this context, we have decided to perform a maximum likelihood estimation of Z_{hh} and Z_{dr} by assuming a bounded variability of all the previous sources of uncertainty. The goal of the maximum likelihood approach has been to render the reconstructed reflectivity profiles, estimated from SPC and GAT radar data, as close as possible along the considered range line. In order to select the optimal estimate of the corrected reflectivity profile $Z_{xx}^{COR}(r)$, we have minimized, with respect to all uncertainties, an error (cost) function E. It is worth remarking that the global minimum of E has been found for a PIA of about 6 dB - with the three correction algorithms indicating a PIA between 5.5 and 6.5 dB - and a calibration-error bias of about 0 dB. Finally, the reconstructed profile has been evaluated by means of the average between the two minimum-error solutions.

The reconstructed Z_{hh} profile is quite close to the composite profile except for the core region between 31 and 36 km where both measured reflectivities are strongly attenuated. The effect of the reconstruction of the Z_{dr} profile is quite similar.

Once the range profiles of Z_{hh} and Z_{dr} have been corrected, the hydrometeor classification algorithm at C-band can be applied. Fig. 2 shows the results obtained by using FRAHCC technique on corrected data. At the lowest radar elevation we are observing the rain core. This emerges from the predominance in Fig. 2 of LD and HR classes with some H/R on the left edge of the storm. As a useful comparison, Fig. 3 shows classification results obtained using reflectivity profiles measured from SPC radar without any path attenuation correction. We note that attenuation correction tends to remove hail regions, provides a continuity of HR and MR, and reduces the presence of LD and NC bins.

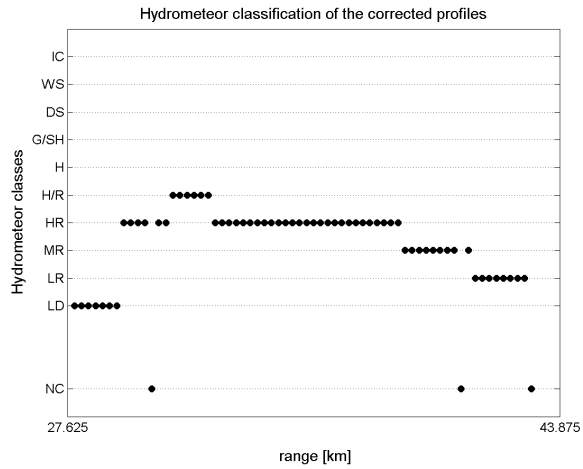

Fig. 2. Hydrometeor classification using FRAHCC applied to the corrected profile.

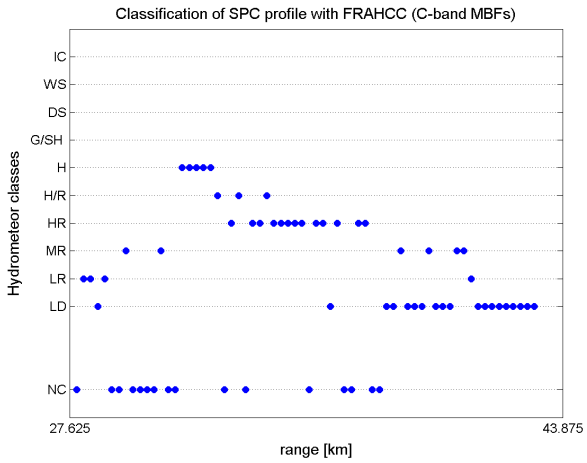

Fig. 3. Hydrometeor classification using FRAHCC applied to SPC data without attenuation correction.

5 Conclusions

Appropriate MBFs, modified for C-band and constituting the basis of FRAHCC approach, have been determined by means of T-Matrix numerical simulations and then tested on synthetic radar data. The overall classification accuracy has considerably increased with respect to the use of S-band MBFs and average not-classified bins percentage has decreased as well. FRAHCC technique has been successively applied to the available radar data, showing accuracy improvements directly visible by observation of the classified RHIs. A path-attenuation correction algorithm, based on either a composite approach or a constrained correction procedure, has been also applied to the entire vertical section of the precipitating cloud. As expected, the impact on hydrometeor classification is noteworthy: final results appear more robust and microphysically consistent.

References

Alberoni, P.P., T. Andersson, P. Mezzasalma, D.B. Michelson, and S. Nanni, 2001: Use of the vertical reflectivity profile for identification of anomalous propagation. *Meteorol. Appl.*, **8**, 257-266.

Alberoni, P.P., L. Ferraris, F.S. Marzano, S. Nanni, R. Pelosini, and F. Siccardi, 2002: The Italian radar network: current status and future developments. *Proc. of ERAD02*, 339-344.

Baldini, L., E. Gorgucci, and V. Chandrasekar, 2004: Hydrometeor classification methodology for C-band polarimetric radars. *Proc. of ERAD04*, 62-66.

Beard, K.V. and D. Chuang, 1987: A New Model for the Equilibrium Shape of Raindrops. *J. Atmos. Sci.*, **44**, 1509–1524.

Bringi, V.N. and V. Chandrasekar, 2001: *Polarimetric Doppler weather radar*, Cambridge University Press, Boston (MA).

Galletti, M., P.P. Alberoni, V. Levizzani, and M. Celano, 2005: Assessment and tuning of the behaviour of a microphysical characterisation scheme. *Adv. in Geosciences*, **2**, 145-150.

Iguchi, T. and R. Meneghini, 1994: Intercomparison of single-frequency methods for retrieving a vertical rain profile from airborne or spaceborne radar data. *J. of Atmos. Oceanic Techn.*, **11**, n. 12, 1507-1516.

Keenan, T.D., 2003: Hydrometeor classification with a C-band polarimetric radar. *Australian Meteor. Mag.*, **52**, n. 1, 23-31.

Lim, S., V. Chandrasekar, and V.N. Bringi, 2005: Hydrometeor classification system using dual-polarization radar measurements: model improvements and in situ verification. *IEEE Trans. Geosci. Rem. Sens.*, **43**, n. 4, 792-801.

Marzano, F.S., D. Scaranari, M. Celano, P.P. Alberoni, G. Vulpiani, M. Montopoli, 2006: Hydrometeor classification from dual-polarized weather radar: extending fuzzy logic from S-band to C-band data. *Adv. in Geosciences*, **7**, 109-114.

Ray, P.S., 1972: Broadband complex refractive indices of ice and water. *Appl. Optics*, **11**, n. 8, 1836-1844.

Ryzhkov, A.V., T.J. Schuur, D.W. Burgess, P.L. Heinselman, S.E. Giangrande, and D.S. Zrnić, 2005: The Joint Polarization Experiment. Polarimetric rainfall measurements and hydrometeor classification. *Bull. Amer. Meteor. Soc.*, **86**, 809-824.

Straka, J.M., D.S. Zrnić, and A.V. Ryzhkov, 2000: Bulk hydrometeor classification and quantification using polarimetric radar data: synthesis of relations. *J. Appl. Met.*, **39**, n. 8, 1341-1372.

Testud, J., E. Le Bouar, E. Obligis, and M. Ali-Mehenni, 2000: The Rain Profiling Algorithm Applied to Polarimetric Weather Radar. *J. Atmos. Oceanic Technol.*, **17**, 332-356.

Vivekanandan, J., D.S. Zrnić, S.M. Ellis, R. Oye, A.V. Ryzhkov, and J. Straka, 1999: Cloud microphysics retrieval using S-band dual-polarization radar measurements. *Bulletin of the American Meteor. Soc.*, **80**, n. 3, 381-388.

Vulpiani, G., F.S. Marzano, V. Chandrasekar and S. Lim, 2005: Constrained iterative technique with embedded neural-network for Dual-Polarization Radar Correction of Rain Path Attenuation. *IEEE Trans. Geosci. Rem. Sensing*, **43**, 2305-2314.

Warren, S.G., 1984: Optical constants of ice from the ultraviolet to the microwave. *Appl. Optics*, **23**, n. 8, 1206-1225.

Zrnić, D.S., A.V. Ryzhkov, J. Straka, Y. Liu, and J. Vivekanandan, 2001: Testing a procedure for automatic classification of hydrometeor types. *J. Atmos. Oceanic Tech.*, **18**, n. 6, 892-913.